

# The CMS ECAL upgrade for the High-Luminosity LHC era

---

**Ka Wa Ho on behalf of the CMS Collaboration<sup>a,\*</sup>**

<sup>a</sup>University of Notre Dame,  
Notre Dame, IN 46556, USA

E-mail: [kho2@nd.edu](mailto:kho2@nd.edu)

The upgraded CERN LHC for high luminosity (HL-LHC) will deliver unprecedented instantaneous luminosities to the detectors which, together with an average of up to 200 simultaneous interactions per bunch crossing, require major upgrades of the CMS electromagnetic calorimeter (ECAL). While a new detector will be installed in the endcap regions, the ECAL barrel lead tungstate crystals and photodetectors are expected to sustain the new conditions. However, a completely new and upgraded readout and trigger electronic system will be installed to cope with the challenging HL-LHC conditions. Each of the 61,200 ECAL barrel crystals will be read out by two custom ASICs providing signal amplification with two gains, ADC with 160 MHz sampling rate, and lossless data compression for the transmission of all channel data to the off-detector electronics. Trigger primitives generation by updated reconstruction algorithms as well as data acquisition will be implemented on powerful FPGAs as a part of the off-detector electronics. The upgrade of the ECAL electronics will maintain the excellent energy resolution of the current detector and, in addition, greatly improve the time resolution of electrons and photons above 10 GeV, down to a few tens of picoseconds. This paper presents the design of the individual components of the upgraded ECAL barrel detector, and results of energy linearity and time resolution measurements with a readout prototype system in a recent test beam campaign at the CERN Super Proton Synchrotron.

*The European Physical Society Conference on High Energy Physics (EPS-HEP2023)  
21-25 August 2023  
Hamburg, Germany*

---

\*Speaker

## 1. The CMS ECAL

The CMS electromagnetic calorimeter (ECAL) is composed of the barrel (EB) and two endcaps (EE). A preshower detector (ES) is installed in front of the endcaps [1]. The EB is made of 61200 lead tungstate crystals, with excellent properties of radiation hardness, short radiation length, and fast scintillation decay time. Each crystal rear-end is equipped with two silicon avalanche photodiodes (APDs) to detect the scintillation light. While the scintillation crystals and APDs will remain unchanged, the EB readout and trigger electronic system will be completely redesigned and upgraded to cope with the LHC for high luminosity (HL-LHC) conditions. A comprehensive technical report on the barrel calorimeter upgrade for the HL-LHC can be found in Ref. [2]. The EE and ES will be replaced by the new high-granularity calorimeter for the HL-LHC.

## 2. The High-Luminosity LHC upgrade

The HL-LHC program, scheduled to start operation in 2029, will deliver a peak instantaneous luminosity of  $5 \times 10^{34} \text{ cm}^{-2}\text{s}^{-1}$ , which is about 2.5 times larger than the current Run 3. The HL-LHC is expected to last 10 years and deliver a total integrated luminosity of at least  $3000 \text{ fb}^{-1}$ . The average number of proton-proton interactions per bunch crossing, also known as pileup events, will increase by up to 4 times the present value to reach an average of about 140–200. The rate of the fast CMS hardware level trigger, or Level-1 (L1) trigger, will increase from the present 100 kHz to about 750 kHz with the latency increasing from  $4.0 \mu\text{s}$  to a max of  $12.5 \mu\text{s}$ .

### 2.1 Challenges of the High-Luminosity LHC at the ECAL barrel

The HL-LHC introduces several challenges for the EB to maintain or to improve the current physics performance. Anomalous signals, or “spikes”, in the EB are generated by the deposition of energy in the depleted silicon bulk of the APDs from heavily ionizing particles. Spikes are characterised by high energy deposits in a single crystal and a fast rising time compared to scintillation signals. The number of spikes increases at a rate proportional to the amount of pileup. The projected fraction of spikes and signals from scintillation at the HL-LHC with 200 pileup events are shown on the left of Fig. 1. If not suppressed, the spikes would saturate the EB L1 bandwidth. Hence, they must be disentangled from genuine signals and rejected at the L1 trigger with a higher efficiency than at present. The dark current in APDs will also increase due to the increased radiation level, leading to the increase of the electronics noise. The EB on-detector electronics will, in addition, have to have to withstand an accumulated irradiation of up to 6 kGy at the end of the HL-LHC.

## 3. The ECAL barrel upgrade for the High-Luminosity LHC

The redesigned electronics will include a new set of on-detector, radiation-hard Very-Front End (VFE) and Front End (FE) cards. The VFE card is composed of five sets of two custom ASICs: the Calorimeter Trans-impedance Amplifier (CATIA) and the Lisboa-Torino ECAL Data Transmission Unit (LiTE-DTU). Each ASIC element will receive signals from a single crystal and a VFE card will be connected to five crystals. Five VFE cards will in turn be connected to a new

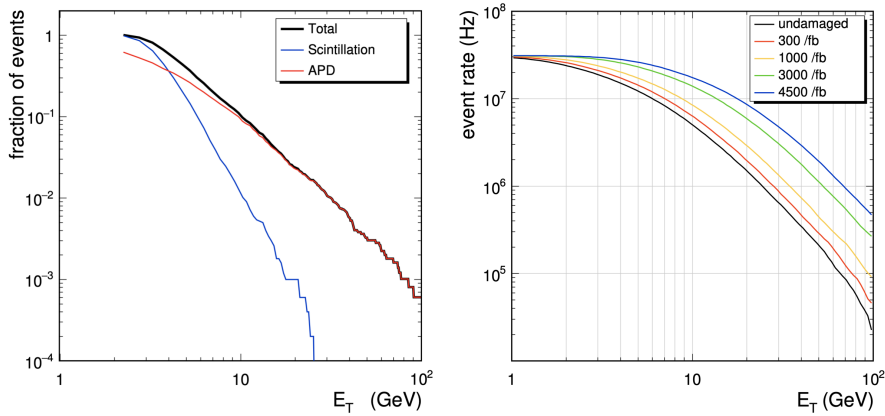


**Figure 1:** Left: fraction of spikes (red) and scintillation signals (blue) expected at the HL-LHC with 200 pileup events. Right: the expected rates of EB energy deposits, including both spikes and scintillation signals, above a given transverse energy threshold at different integrated luminosities at the HL-LHC.

FE card. A new off-detector electronics board, the Barrel Calorimeter Processor (BCP) board, will also be available, connecting to 24 FE cards (600 crystals).

The redesigned on-detector electronics will be able to withstand the radiation level foreseen at the HL-LHC; the increase in electronics noise due to the increase of the APD dark current will be controlled by lowering the operating temperature from 18 °C to 9 °C. The data sampling rate of the EB crystal data will be increased to 160 MHz to facilitate the rejection of spikes at the L1 trigger. With the increased sampling rate, an improved timing resolution of about 30 ps is expected for signals with energy above 50 GeV.

### 3.1 Very-Front End card

#### 3.1.1 Calorimeter Transimpedance Amplifier

The CATIA is a dual gain circuit transimpedance amplifier. The gain 10 (gain 1) is designed for a low (high) energy range from 50 MeV to 200 GeV (2 TeV) with a resolution of 50 MeV (500 MeV). The CATIA has a small intrinsic noise of 80 MeV and a bandwidth twice the current system of up to 50 MHz to facilitate the spike rejection at the L1 trigger. It also has an excellent integral non-linearity of  $\pm 1/1000$  for the full scale of energy. This property is demonstrated by Fig. 2 showing the uniformity of signal pulse shapes recorded from a crystal equipped with the new VFE card exposed to electron beams with energies of 25–150 GeV (see Sec. 4). In addition, the CATIA also provides a reference voltage for ADC calibration and pedestal tuning, a temperature sensor, and the functionality to inject test pulse for system monitoring.

#### 3.1.2 Lisboa-Torino ECAL Data Transmission Unit

The LiTE-DTU digitizes the two CATIA outputs to two 12-bit ADC samples at 160 MHz. The Data Control and Transmission Unit of the LiTE-DTU performs the gain selection and data compression of the samples. For the gain selection, gain 10 is selected by default for its higher energy resolution. When gain 10 is saturated, gain 1 will be selected for a window of eight samples

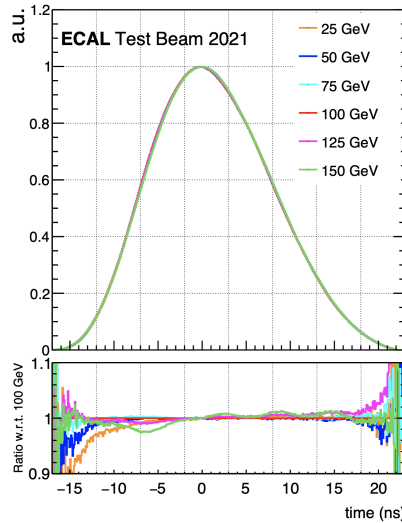


**Figure 2:** Signal pulses generated in a single crystal with the upgraded VFE in a 2021 test beam. The pulse shapes can be seen to be uniform across a wide range of electron beam energies of 25–150 GeV, demonstrating the integral non-linearity of the CATIA.

or more, depending on the number of saturated samples. Each uncompressed sample is represented by 13 bits in total, with 12 bits for the amplitude and 1 bit for the gain selected.

The hit energy spectrum of EB falls rapidly and the majority of the samples will consist of noise or low-energy signals. The expected event rates of EB above a given transverse energy threshold are plotted on the right of Fig. 1 at different integrated luminosities of the HL-LHC. It is estimated that the probability of having a sample with more than 6 significant bits is  $< 2.4 \times 10^{-4}$ . Hence, data samples are compressed with a simplified lossless Huffman encoding algorithm [3] from 2.08 Gb/s to fit in a single 1.28 Gb/s serial link; 6 bits are used to encode samples of up to 2.5 GeV and 12 bits are used for energy above.

### 3.2 Front End card

The FE card serves as an interface between the BCP and the VFE cards. CERN-developed, radiation and magnetic field tolerant electronics components for the HL-LHC are used on the FE card, including the high speed optical Versatile Link Plus Transceiver, the Low Power GigaBit Transceiver, and the GigaBit-Slow Control Adapter. Slow controls and VFE data are transceived via five optical links. These include one receiving link from the BCP at 2.56 Gb/s to distribute the LHC clock and control information, and four transmitting links to the BCP at 10.24 Gb/s to transmit the VFE data and status, such as the VFE temperature and the APD leakage current.

### 3.3 Barrel Calorimeter Processor

The BCP is responsible for the LHC clock and control distribution to the FE, data decompression, trigger primitive generations (TPG), and data transmission to the CMS L1 trigger and data acquisition system. The main processing power of the board is provided by a FPGA to carry out the data decompression and TPG. An Embedded Linux Mezzanine with the PetaLinux environment is used as the main controller of the board. The Intelligent Platform Management Controller on the

board controls and sequences power up of all power modules. It also monitors the temperatures and power rails of the BCP. In case of failure, it is able to cut off the power in  $< 400 \mu\text{s}$ .

### 3.3.1 Trigger primitive generation algorithms

The TPG algorithms will be implemented as a part of the firmware on the FPGA of the BCP. The digitized samples from the Lite-DTU are first multiplied by their gain and the pedestal is subtracted to be linear to the transverse energy measured. A linear least squares method, using predetermined (templated) pulse shapes of crystals is used to extract the amplitude and timing of signals, taking into account a possible overlay of signals from the  $\pm 1$  bunch crossings. Thanks to the fast shaping time (about 20 ns) of the CATIA chip, and the high (160 MHz) sampling rate, spikes are expected to be identified effectively based on a discriminant,  $LD$ , built from the ratios of three consecutive linearized samples ( $a_{i-1}, a_i, a_{i+1}$ ):

$$LD = \frac{a_{i+1}}{a_i} - \sum_{j=0}^3 p_j \times \frac{a_{i-1}^j}{a_i^j}, \quad (1)$$

where  $p_j$  are parameters from a third order polynomial fit to the signal pulse shape. The average spike and scintillation signal shapes expected at the 160 MHz sampling rate are shown on the left of Fig. 3. The distributions of  $LD$  expected for spikes and scintillation signals are shown on the right of Fig. 3 in the case when the amplitudes are 50 times the noise. It can be seen that  $LD$  offers an excellent discrimination between the spikes and signals.

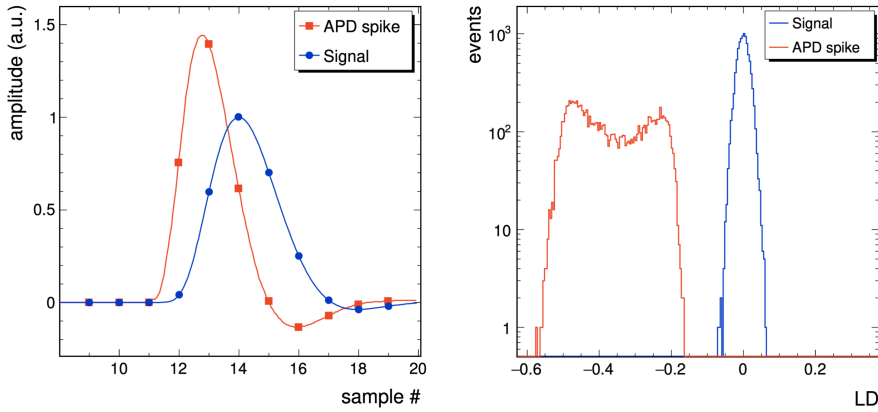


**Figure 3:** Left: average spike (red) and scintillation signal (blue) shape expected at the 160 MHz sampling rate. Right: distribution of the pulse shape discriminant,  $LD$ , expected for spikes (red) and scintillation signals (blue) with amplitudes 50 times the noise.

## 4. Test beam results

A test beam was carried out in 2021 with 25 crystals equipped with 5 VFE cards and a custom readout. Electron beams of 25–150 GeV in step of 25 GeV were used in the test beam at the CERN Super Proton Synchrotron. Plastic fiber hodoscopes were used to determine the beam position with

a resolution of around  $1 \times 1 \text{ mm}^2$ , compared to the crystal front face area of  $2 \times 2 \text{ mm}^2$ . Micro channel plates (MCPs) were used as a precise timing reference with a resolution of around 14 ps.

The average reconstructed energy expressed in ADC counts of a single channel of crystal as a function of the electron beam energy is shown in Fig. 4 (left). It can be seen that with the upgraded VFE card the ADC response demonstrates an excellent linearity to the beam energy with  $< 0.3\%$  deviation. Fig. 4 (right) shows the time resolution of a single channel obtained comparing the crystal time to the reference time of the MCPs as a function of the deposited energy. The expectation of a 30 ps time resolution for energy  $> 50 \text{ GeV}$  is met.

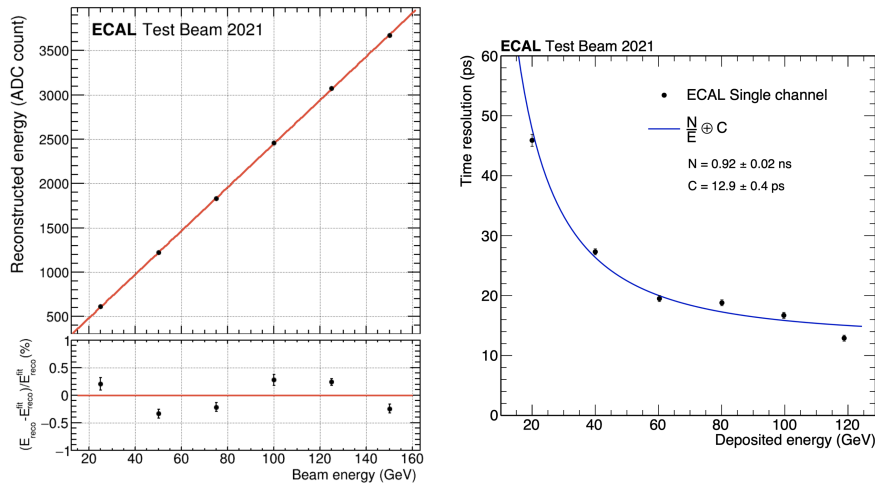


**Figure 4:** The energy linearity and timing resolution of the redesigned VFE card demonstrated from the 2021 test beam data. The average reconstructed energy expressed in ADC counts of a single channel of crystal as a function of the electron beam energy is shown on the left. The time resolution of a single channel obtained comparing the crystal time to the reference time of the MCPs is shown on the right as a function of the deposited energy.

## 5. Conclusion

The CMS EB readout and back-end electronics will be completely re-designed and upgraded for the HL-LHC. This includes a VFE card with two new custom ASICs, a new FE card, and a new off-detector electronics processor. The overall upgrade is aiming to cope with the increased L1 trigger rate, latency, and pileup at CMS, and the increased APD dark current at EB. It also aims at preserving the EB energy resolution achieved during Run 1 to Run 3 and achieving a better time resolution, despite the harsh changes in conditions expected for the HL-LHC. Studies on test beam carried out so far, show very promising results on the pulse shape uniformity, energy linearity, and timing resolution with the new VFE electronics.

## References

- [1] CMS Collaboration, “The CMS experiment at the CERN LHC”, *JINST* **3** (2008) S08004, [doi:10.1088/1748-0221/3/08/S08004](https://doi.org/10.1088/1748-0221/3/08/S08004).

- [2] CMS Collaboration, “The Phase-2 Upgrade of the CMS Barrel Calorimeters”, Technical Report CERN-LHCC-2017-011, CERN, Geneva, 2017.  
<https://cds.cern.ch/record/2283187>.
- [3] D. A. Huffman, “A method for the construction of minimum-redundancy codes”, *Proceedings of the IRE* **40** (1952), no. 9, 1098, doi : 10.1109/JRPROC.1952.273898.